First measurement of the vertical bar t vertical bar-dependence
of coherent J/psi photonuclear production

The ALICE collaboration

2021-06-10

First measurement of the $|t|$-dependence of coherent J/ψ photonuclear production

ALICE Collaboration ⋆

ABSTRACT

The first measurement of the cross section for coherent J/ψ photoproduction as a function of $|t|$, the square of the momentum transferred between the incoming and outgoing target nucleus, is presented. The data were measured with the ALICE detector in ultra-peripheral Pb–Pb collisions at a centre-of-mass energy per nucleon pair $\sqrt{s_{NN}} = 5.02$ TeV with the J/ψ produced in the central rapidity region $|y| < 0.8$, which corresponds to the small Bjorken-x range $(0.3 - 1.4) \times 10^{-3}$.

The measured $|t|$-dependence is not described by computations based only on the Pb nuclear form factor, while the photonuclear cross section is better reproduced by models including shadowing according to the leading-twist approximation, or gluon-saturation effects from the impact-parameter dependent Balitsky–Kovchegov equation. These new results are therefore a valid tool to constrain the relevant model parameters and to investigate the transverse gluonic structure at very low Bjorken-x.

© 2021 The Author(s). Published by Elsevier B.V. This is an open access article under the CC BY license (http://creativecommons.org/licenses/by/4.0/). Funded by SCOAP³.

1. Introduction

Photonuclear reactions can be studied in ultra-peripheral collisions (UPCs) of heavy ions where the two projectiles pass each other with an impact parameter larger than the sum of their radii. In this case, purely hadronic interactions are suppressed and electromagnetically induced processes occur via photons with typically very small virtualities, of the order of tens of MeV². The intensity of the photon flux is proportional to the square of the electric charge of the nuclei, resulting in large cross sections for the coherent photoproduction of a vector meson in UPCs of Pb ions at the LHC. This process has a clear experimental signature: the decay products of the vector meson are the only particles detected in an otherwise empty detector.

The physics of vector meson photoproduction is described, e.g., in Refs. [1–4]. Two vector meson photoproduction processes, coherent and incoherent, are relevant for the results presented here. In the former, the photon interacts with all nucleons in a nucleus, while in the latter it interacts with a single nucleon. In both cases a single vector meson is produced. Experimentally, one can distinguish between these two production types through the transverse momentum p_{T} of the vector meson which is related to the transverse size of the target. While coherent photoproduction is characterised by an average transverse momentum $\langle p_{\mathrm{T}} \rangle \sim 60$ MeV/c, incoherent production leads to higher average transverse momenta: $\langle p_{\mathrm{T}} \rangle \sim 500$ MeV/c. Incoherent photoproduction can also be accompanied by the excitation and dissociation of

the target nucleon resulting in an even higher transverse momentum of the produced vector meson [5].

Shadowing, the observation that the structure of a nucleon inside nuclear matter is different from that of a free nucleon [6], is not yet completely understood and several processes may have a role in different kinematic regions. In this context, coherent heavy vector meson photoproduction is of particular interest, because it is especially sensitive to the gluon distribution in the target, and thus to gluon shadowing effects at low Bjorken-x [7,8]. One of the effects expected to contribute to shadowing in this kinematic region is saturation, a dynamic equilibrium between gluon radiation and recombination [9]. The momentum scale of the interaction (Q^2) is related to the mass m_V of the vector meson as $Q^2 \sim m_V^2/4$, corresponding to the perturbative regime of quantum chromodynamics (QCD) in the case of charmonium states. The rapidity of the coherently produced $c\bar{c}$ states is related to the Bjorken-x of the gluonic exchange as $x = \left(m_V / \sqrt{s_{NN}}\right) \exp(\pm y)$, where the two signs indicate that either of the incoming ions can be the source of the photon. Thus, the charmonium photoproduction cross section at midrapidity in Pb–Pb UPCs at the LHC Run 2 centre-of-mass energy per nucleon pair of $\sqrt{s_{NN}} = 5.02$ TeV is sensitive to $x \in (0.3, 1.4) \times 10^{-3}$ at ALICE. It thereby provides information on the gluon distribution in nuclei in a kinematic region where shadowing could be present and saturation effects may be important [10,11].

Charmonium photoproduction in ultra-peripheral Pb–Pb collisions was previously studied by the ALICE Collaboration at $\sqrt{s_{NN}} = 2.76$ TeV [12–14]. The coherent J/ψ photoproduction cross section was measured both at midrapidity $|y| < 0.9$ and at forward

⋆ E-mail address: alice-publications@cern.ch.

rapidity $-3.6 < y < -2.6$. Recently, a measurement of the rapidity dependence of coherent J/ψ photoproduction at forward rapidity at the higher energy of $\sqrt{s_{NN}} = 5.02$ TeV was also published by the ALICE Collaboration [15]. In addition, the CMS Collaboration studied the coherent J/ψ photoproduction accompanied by neutron emission at semi-forward rapidity $1.8 < |y| < 2.3$ at $\sqrt{s_{NN}} = 2.76$ TeV [16]. These measurements allow for a deeper insight into the rapidity dependence of gluon shadowing, but do not give information on the behaviour of gluons in the impact-parameter plane. The square of the momentum transferred to the target nucleus, $|t|$, is related through a two-dimensional Fourier transform to the gluon distribution in the plane transverse to the interaction [17]; thus the study of the $|t|$-dependence of coherent J/ψ photoproduction provides information about the spatial distribution of gluons as a function of the impact parameter. Thus far, the only measurements in this direction were performed recently by the STAR Collaboration for the case of the ρ^0 vector meson [18] and for the yield of J/ψ in semi-central Au–Au collisions [19].

In this Letter, the first measurement of the $|t|$-dependence of the coherent J/ψ photoproduction cross section at midrapidity in Pb–Pb UPCs at $\sqrt{s_{NN}} = 5.02$ TeV is presented. The J/ψ vector mesons were reconstructed in the rapidity range $|y| < 0.8$ through their decay into $\mu^+\mu^-$, taking advantage of the better mass and momentum resolution of this channel with respect to the e^+e^- channel. The data sample, recorded in 2018, is approximately 10 times larger than that used in previous ALICE measurements at midrapidity at the lower energy of $\sqrt{s_{NN}} = 2.76$ TeV [14]. Cross sections are reported for six $|t|$ intervals and compared with theoretical predictions.

2. Detector description

The ALICE detector and its performance are described in Refs. [20,21]. Three central barrel detectors, the Inner Tracking System (ITS), the Time Projection Chamber (TPC), and the Time-of-Flight (TOF), in addition to two forward detectors, V0 and the ALICE Diffractive (AD) arrays, are used in this analysis. The central barrel detectors are surrounded by a large solenoid magnet producing a magnetic field of $B = 0.5$ T. The V0, AD, ITS, and TOF detectors are used for triggering, the ITS and the TPC for particle tracking, and the TPC for particle identification.

The V0 is a scintillator detector made of two counters, V0A and V0C, installed on both sides of the interaction point. The V0A and V0C cover the pseudorapidity ranges $2.8 < \eta < 5.1$ and $-3.7 < \eta < -1.7$, respectively. Both counters are segmented in four rings in the radial direction, with each ring divided into 8 sections in azimuth.

The AD consists of two scintillator stations, ADA and ADC, located at 16 and -19 m along the beam line with respect to the nominal interaction point and covering the pseudorapidity ranges $4.8 < \eta < 6.3$ and $-7.0 < \eta < -4.9$, respectively [22,23].

The ITS is a silicon based detector and is made of six cylindrical layers using three different technologies. The Silicon Pixel Detector (SPD) forms the two innermost layers of the ITS and covers $|\eta| < 2$ and $|\eta| < 1.4$, respectively. Apart from tracking, the SPD is also used for triggering purposes and to reconstruct the primary vertex.

The ITS is cylindrically surrounded by the TPC, whose main purpose is to track particles and provide charged-particle momentum measurements with good two-track separation and particle identification. The TPC coverage in pseudorapidity is $|\eta| < 0.9$ for tracks with full radial length. The TPC has full coverage in azimuth. It offers good momentum resolution in a large range of the track transverse momentum spanning from 0.1 GeV/c to 100 GeV/c.

The TOF is a large cylindrical gaseous detector based on multi-gap resistive-plate chambers. It covers the pseudorapidity region $|\eta| < 0.8$. The TOF readout channels are arranged into 18 azimuthal sectors which can provide topological trigger decisions.

3. Data analysis

3.1. Event selection

The online event selection was based on a dedicated UPC trigger which selected back-to-back tracks in an otherwise empty detector. This selection required (i) that nothing above the trigger threshold was detected in the V0 and AD detectors, (ii) a topological trigger requiring less than eight SPD chips with trigger signal, forming at least two pairs; each pair was required to have an SPD chip fired in each of the two layers and to be in compatible azimuthal sectors, with an opening angle in azimuth between the two pairs larger than 144°, (iii) a topological trigger in the TOF requiring more than one and less than seven TOF sectors to register a signal; at least two of these sectors should have an opening angle in azimuth larger than 150°.

The integrated luminosity of the analysed sample is 233 μb^{-1}. The determination of the luminosity is obtained from the counts of a reference trigger based on multiplicity selection in the V0 detector, with the corresponding cross section estimated from a van der Meer scan; this procedure has an uncertainty of 2.2% [24]. The determination of the live-time of the UPC trigger has an additional uncertainty of 1.5%. The total relative systematic uncertainty of the integrated luminosity is thus 2.7%.

Additional offline V0 and AD veto decisions were applied in the analysis. The offline veto algorithm improved the signal to background ratio, because it utilised a larger timing window to integrate the signal than its online counterpart. Some good events were lost due to this selection. The loss was taken into account with the correction on veto trigger inefficiency discussed in Sec. 3.4. The systematic uncertainty from the V0 and AD vetoes was estimated as the relative change in the measured J/ψ cross section before and after imposing them and correcting for the losses; it amounts to 3%.

Each event had a reconstructed primary vertex within 15 cm from the nominal interaction point along the beam direction, z, and had exactly two tracks. These tracks were reconstructed using combined tracking in the ITS and TPC. Tracks were requested to have at least 70 (out of 159) TPC space points and to have a hit in each of the two layers of the SPD. Each track had to have a distance of closest approach to the event interaction vertex of less than 2 cm in the z-axis direction. Also, each track was required to have $|\eta| < 0.9$. The relative systematic uncertainty from tracking, which takes into account the track quality selection and the track propagation from the TPC to the ITS, was estimated from a comparison of data and Monte Carlo simulation. The combined uncertainty to reconstruct both tracks is 2.8%.

The particle identification (PID) was provided by the specific ionisation losses in the TPC, which offer a large separation power between muons and electrons from the leptonic decays of the J/ψ in the momentum range $(1.0, 2.0)$ GeV/c, relevant for this analysis. The effect of a possible misidentification was found to be negligible.

An offline SPD decision was also applied in the analysis. The offline topological SPD algorithm ensured that the selected tracks crossed the SPD chips used in the trigger decision. The relative systematic uncertainty from the SPD and TOF trigger amounts to 1.3%, which was estimated using a data-driven method by changing the requirements on the probe tracks.

The selected events were required to have tracks with opposite electric charge, the rapidity of the dimuon candidate was restricted to $|y| < 0.8$ and its p_T had to be less than 0.11 GeV/c, in order to obtain a sample dominated by coherent interactions

with just a small contamination from incoherent processes. The measurement was initially carried out in p_T^2 intervals, because for collider kinematics $|t| \approx p_T^2$. The corrections needed to obtain the $|t|$-dependence are discussed in Sec. 3.7.

3.2. Signal extraction

As a first step in extracting the coherent J/ψ signal, a fit to the opposite sign dimuon invariant mass distribution was performed. The model used to fit the data consists of three templates: one Crystal Ball function [25] (CB) to describe the J/ψ resonance, a second CB function to describe the ψ' resonance, and an exponential function to describe the continuum production of muon pairs, $\gamma\gamma \to \mu^+\mu^-$.

The parameters of the exponential function were left free. The integral of this exponential in the mass range $(3.0, 3.2)$ GeV/c^2 was used to determine the number of events from the continuum production in this interval.

The CB parameters describing the tails of the measured distribution in data, commonly known as α and n, were fixed to the values obtained while fitting the dimuon invariant mass distribution in an associated Monte Carlo simulation, which is described in Sec. 3.4. These settings were employed for both CB functions.

The number of J/ψ candidates in each p_T^2 interval was obtained from an extended maximum likelihood fit to the unbinned invariant mass distribution of all $\mu^+\mu^-$ pairs which survived the selection criteria described in Sec. 3.1. Results of the fits for the six p_T^2 intervals are shown in Fig. 1. In all cases a very clear J/ψ resonance is seen over a fairly small background. Note that the effect on the kinematics from a potential dimuon decay including bremsstrahlung is negligible.

The relative systematic uncertainty from the signal extraction was calculated by repeating the fit over different invariant mass ranges, and modifying the CB α and n parameters accordingly. These uncertainties vary in the interval (0.7,2.2)%.

3.3. Corrections for irreducible backgrounds

The selection criteria described above are not sensitive to events which mimic the signature of coherent J/ψ production, but are coming from feed-down of ψ' or incoherent production. The contribution of these events was taken into account with the f_D and f_I factors, respectively, entering Eq. (1),

$$N_{J/\psi}^{coh} = \frac{N^{fit}}{1 + f_I + f_D} \times \frac{1}{(Acc \times \varepsilon)_{J/\psi}^{coh}}, \tag{1}$$

where N^{fit}, the yield of J/ψ candidates, is the integral of the CB describing the J/ψ signal in the fit of the dimuon invariant mass spectrum, and $(Acc \times \varepsilon)_{J/\psi}^{coh}$ is the acceptance and efficiency correction factor described in Sec. 3.4.

Feed-down refers to the decay of a ψ' to a J/ψ plus anything else, where these additional particles were not detected for some reason. The correction for these events, f_D, was estimated with Monte Carlo simulations describing the apparatus (Acc $\times \varepsilon$) factor for the following channels: J/$\psi \to \mu^+\mu^-$, $\psi' \to \mu^+\mu^-$, and $\psi' \to$ J/$\psi + X$; and the measured ratio of ψ' to J/ψ production cross sections. The details of the method are described in Ref. [15]. The results for each p_T^2 interval are summarised in Table 1. Relative systematic uncertainties, estimated by using different cross section ratios, are p_T^2-correlated. Their relative effect on the final cross section can be found in Table 2; it is well below 1%.

Most of the incoherent production of J/ψ off nucleons was rejected with the restriction of the phase space in p_T, as mentioned in Sec. 3.1. However, around 5% of all incoherent events remained

Table 1

Incoherent correction f_I, feed-down correction f_D and the $(Acc \times \varepsilon)_{J/\psi}^{coh}$ correction factor for each p_T^2 interval. See Eq. (1).

| p_T^2 interval (GeV^2/c^2)	f_I	f_D	$(Acc \times \varepsilon)_{J/\psi}^{coh}$
(0, 0.00072)	0.0045	0.0039	0.0348
(0.00072, 0.0016)	0.0047	0.0046	0.0352
(0.0016, 0.0026)	0.0047	0.0058	0.0358
(0.0026, 0.004)	0.0072	0.0072	0.0365
(0.004, 0.0062)	0.0120	0.011	0.0379
(0.0062, 0.0121)	0.0300	0.028	0.0412

Table 2

Summary of the identified systematic uncertainties on the coherent J/ψ photoproduction and photonuclear cross sections. The uncertainties to go from the measured cross section in UPCs to the photonuclear process are listed after the line in the middle of the table and their origin depends on the modeling of the photon flux and interference effects. The correlation across p_T^2 intervals is discussed in the text.

Source	Uncertainty (%)
Signal extraction	(0.7, 2.2)
f_D	(0.1, 0.5)
f_I	(1.1, 2.3)
p_T^2 migration unfolding	(0.6, 2.3)
Luminosity	2.7
V0 and AD veto	3
EM dissociation	2
ITS-TPC tracking	2.8
SPD and TOF efficiency	1.3
Branching ratio	0.5
Variations in interference strength	(0.3, 1.2)
Value of the photon flux at $y = 0$	2
$p_T^2 \to |t|$ unfolding	(0.1, 5.7)

in the region where the measurement was performed. To estimate the f_I factor to correct for the remaining incoherent events, a fit to the measured J/ψ p_T distribution of data in the invariant mass range $(3.0, 3.2)$ GeV/c^2 was used. The model fitted to the data consists of six templates: coherent J/ψ photoproduction, incoherent J/ψ photoproduction, incoherent J/ψ photoproduction with nucleon dissociation, coherent ψ' photoproduction, incoherent ψ' photoproduction, and continuum production from $\gamma\gamma \to \mu^+\mu^-$. The templates of all, but dissociative J/ψ and continuum, were taken from Monte Carlo simulations. In the fit, the fractions of both ψ' photoproduction processes were fixed to values calculated as described above. These included the modifications that the p_T restriction was released and that there was a selection on the invariant mass to be in the range $(3.6, 3.8)$ GeV/c^2. Other fractions were left free in the fit. The normalisation of the continuum was restricted from the invariant mass fit to be the sum of background events in the mass range of the J/ψ. The shape of the continuum was taken from the dimuon p_T distribution selecting the invariant mass range between the J/ψ and the ψ', while the shape for the nucleon dissociation process was based on the H1 parameterisation [26]. The global template was fitted to data using an extended maximum likelihood unbinned fit. The results for each p_T^2 interval are reported in Table 1. The systematic uncertainties, estimated from a combination of the fit uncertainty and a modification of the coherent template used in the fitting model are p_T-correlated. Their relative effect on the final cross section can be found in Table 2.

3.4. Acceptance, efficiency and pile-up corrections

The STARlight 2.2.0 MC generator [27] was used to generate samples of coherent and incoherent events for the production of J/$\psi \to \mu^+\mu^-$ and $\psi' \to \mu^+\mu^- + \pi^+\pi^-(\pi^0\pi^0)$. GEANT 3.21 [28]
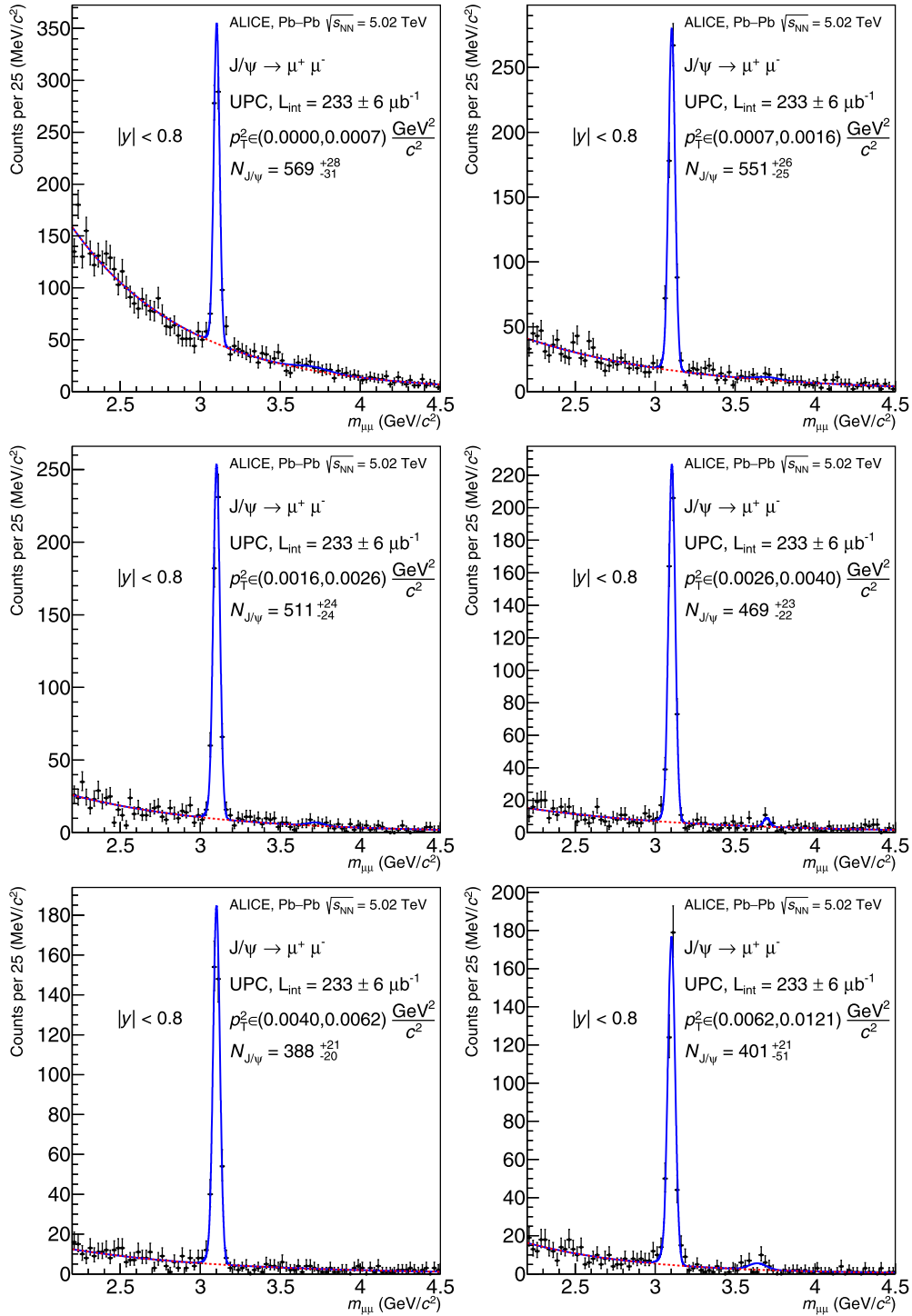
Fig. 1. Invariant-mass distributions for different p_T^2 intervals with the global fit described in the text shown with the blue line. The exponential part of the fit model, representing the $\gamma\gamma \to \mu^+\mu^-$ background, is shown in red.

was used to reproduce the response of the detector. The simulated data were reconstructed with the same software as the real ones, accounting for actual data-taking conditions. Values of the acceptance and efficiency, $(\text{Acc} \times \varepsilon)_{J/\psi}^{\text{coh}}$, are shown in Table 1 for the different p_T^2 intervals used in this analysis.

AD and V0 were used to veto activity at forward rapidity. These detectors were sensitive to signals coming from independent interactions (pile-up), which resulted in the rejection of potentially interesting events. The correction factor for this effect was obtained using a control sample of events collected with an unbiased

trigger. These were then used to compute the probability of having a veto from AD or V0 in otherwise empty events. The total veto trigger efficiency $\varepsilon^{\text{VETO}}$ used in Eq. (2) was determined to be 0.94. The corresponding systematic uncertainty is included in the AD and V0 value of 3% mentioned in Sec. 3.1.

Electromagnetic dissociation (EMD) is another process which may cause the rejection of a good event due to the veto from the forward detectors. EMD can occur when photons excite one or both interacting nuclei. Upon de-excitation, neutrons and sometimes other charged particles are emitted at forward rapidities [29]

and can trigger a V0 or AD veto. Such loss of events was quantified from data gathered with a specialized EMD trigger; the efficiency correction factor to take into account these losses amounts to $\varepsilon^{\text{EMD}} = 0.92$ with a relative systematic uncertainty of 2% given by the statistical uncertainty from the control sample.

3.5. Unfolding of the p_{T}^2 distribution

Cross sections were measured in different p_{T}^2 intervals. In order to account for the migration of about 45% of the events across p_{T}^2 intervals due to the finite resolution of the detector, an unfolding procedure was used. The effect of migrations are much more important than the small difference between the data and MC p_{T} spectra, so no re-weighting has been performed previous to unfolding.

Amongst many available methods, unfolding based on Bayes' theorem [30] was chosen to perform the unfolding, while the singular-value decomposition (SVD) method [31] served to study potential systematic effects. The implementations of these methods as provided by RooUnfold [32] were used in this analysis.

Bayesian unfolding is an iterative method, therefore the result depends on the number of iterations. The size of the data sample is large enough to investigate different numbers of p_{T}^2 ranges. These two parameters, that is the number of iterations and of ranges, were tuned using Monte Carlo simulations by studying the evolution of the statistical uncertainty in each interval as a function of the number of iterations, and by using the relative difference between iteration-adjacent results. It was found that the best combination for this analysis is Bayes' unfolding with three iterations applied to the p_{T}^2 distribution split into six regions. The widths of the p_{T}^2 intervals were chosen to have similar statistical uncertainties in each region.

The Monte Carlo sample used for unfolding contained 600 000 events. An 80% fraction of them was used to train the response matrix which is used to unfold the true distribution from the measured distribution. This matrix was tested on the remaining 20% of the events. The unfolding matrix was able to correct the smeared distribution with high precision. Comparison with results using the SVD method revealed a p_{T}-correlated relative systematic uncertainty with values in the interval (0.6, 2.3)%.

3.6. Cross section for coherent J/ψ photoproduction in UPCs

The differential cross section for coherent J/ψ photoproduction in a given p_{T}^2 interval and a given rapidity range Δy in Pb–Pb UPCs is

$$\frac{\text{d}^2\sigma_{\text{J}/\psi}^{\text{coh}}}{\text{d}y\text{d}p_{\text{T}}^2}$$

$$= \frac{{}^{\text{unf}}N_{\text{J}/\psi}^{\text{coh}}}{\varepsilon^{\text{VETO}} \times \varepsilon^{\text{EMD}} \times \text{BR(J}/\psi \to \mu^+\mu^-) \times \mathscr{L}_{\text{int}} \times \Delta p_{\text{T}}^2 \times \Delta y}, \tag{2}$$

where the correction factors $\varepsilon^{\text{VETO}}$ and ε^{EMD} are introduced in Sec. 3.4, BR(J/$\psi \to \mu^+\mu^-$) is the branching ratio (5.961 $\pm$ 0.033)% [33], $\mathscr{L}_{\text{int}}$ is the total integrated luminosity of the data sample, Δp_{T}^2 is the size of the interval where the measurement was performed, and finally, ${}^{\text{unf}}N_{\text{J}/\psi}^{\text{coh}}$ is the number of coherent J/ψ candidates after unfolding the results given by Eq. (1). The corresponding systematic uncertainties are summarised in the upper part of Table 2. With the exception of signal extraction, all other systematic uncertainties mentioned up to here are correlated across p_{T}^2 intervals.

3.7. Corrections for the photonuclear cross section

The cross section described by Eq. (2) is the one measured by ALICE. The main theoretical interest is in the photonuclear process at a fixed energy. To obtain the corresponding cross section, one has to account for several effects. None of these effects is affected by the ALICE detector, they just depend on the kinematics and quantum nature of the process. This means that the uncertainties in going from the UPC to the photonuclear cross sections are of theoretical nature only.

At midrapidity, the UPC cross section corresponds to the γPb cross section multiplied by twice the photon flux averaged over the impact parameter, $n_{\gamma\text{Pb}}(y)$,

$$\left.\frac{\text{d}^2\sigma_{\text{J}/\psi}^{\text{coh}}}{\text{d}y\text{d}p_{\text{T}}^2}\right|_{y=0} = 2n_{\gamma\text{Pb}}(y=0)\frac{\text{d}\sigma_{\gamma\text{Pb}}}{\text{d}|t|}. \tag{3}$$

Since the rapidity dependence of the UPC cross section in the rapidity range studied here is fairly flat, the measurements are taken to represent the value at $y = 0$. In UPCs, there are two potential photon sources, so in principle both amplitudes have to be added and their interference needs to be accounted. This was studied for the first time in Ref. [34] and later measured for the case of ρ^0 coherent photoproduction by the STAR Collaboration [35]. The interference is important only at very small values of $|t|$ (see for example [36]). To account for this effect, the STARlight program, which includes the interference of both amplitudes, was used. It was found that this is an 11.6% effect in the smallest $|t|$ interval, where the effect is concentrated. To estimate the potential uncertainty on this procedure, the interference effects with the nominal strength were compared to those with a 25% reduction of the strength. The relative change in the photonuclear cross section varied from 0.3 to 1.2% with the largest uncertainty being assigned to the smallest $|t|$ interval.

The photon flux was computed in the semiclassical formalism following the prescription detailed in Ref. [37] and cross checked with that of Ref. [38]. The flux amounts to 84.9 with an uncertainty of 2% coming from variations of the geometry of the Pb ions.

Although the value of p_{T}^2 is a good approximation to that of $|t|$, it is not exact due to the fact that the photon also has a transverse momentum in the laboratory frame. To account for this effect, the cross section was unfolded with a response matrix built from p_{T}^2- and $|t|$-distributions. Two sources for the distributions were used: (*i*) the STARlight generator which includes the transverse momenta of the photons, but does not describe so well the shape of the measured p_{T}^2 distribution in data, and (*ii*) measured p_{T}^2 values coupled to photon momenta randomly generated using the transverse momentum distribution of photons from Refs. [39,40]. The average of the corresponding unfolded results was used for the cross section, while half their difference was taken as a systematic uncertainty which varied between 0.1% and 5.7%, with this last value corresponding to the largest $|t|$ interval.

These three uncertainties are reported in the lower part of Table 2. The uncertainty on the value of the photon flux at $y = 0$ is correlated across $|t|$, the uncertainty on the $p_{\text{T}}^2 \to |t|$ unfolding is partially correlated and the uncertainty on the variation of the interference term is anti-correlated in the lowest $|t|$ region and correlated in the other $|t|$ regions. They are added in quadrature for the final result shown in Sec. 4 and Table 3 below.

4. Results

The final result for the cross section measured in each p_{T}^2 interval is reported in Table 3. The statistical uncertainty originates from the error obtained in the fit to the dimuon invariant-mass

Table 3

Measured coherent J/ψ photoproduction cross section in UPCs in different p_T^2 intervals as well as the photonuclear cross section in $|t|$-intervals. The first uncertainty is statistical, the second and third systematic, uncorrelated and correlated, respectively. The fourth uncertainty, for the photonuclear cross section case, is the systematic uncertainty on the correction to go from the UPC to the photonuclear cross section. The mean value of $|t|$ in each interval is also shown.

Interval (GeV$^2c^{-2}$)	$\langle|t|\rangle$ (GeV$^2c^{-2}$)	$\frac{d^2\sigma_{J/\psi}^{coh}}{dy\,dp_T^2}$ ($\frac{mbc^2}{GeV^2}$)	$\frac{d\sigma_{\gamma Pb}}{d|t|}$ ($\frac{mbc^2}{GeV^2}$)
$(0, 0.72) \times 10^{-3}$	0.00032	$1290 \pm 74 \pm 29 \pm 73$	$8.15 \pm 0.50 \pm 0.18 \pm 0.46 \pm 0.20$
$(0.72, 1.6) \times 10^{-3}$	0.00113	$1035 \pm 47 \pm 10 \pm 60$	$5.75 \pm 0.27 \pm 0.06 \pm 0.34 \pm 0.16$
$(1.6, 2.6) \times 10^{-3}$	0.00207	$743 \pm 34 \pm 6 \pm 43$	$4.23 \pm 0.20 \pm 0.03 \pm 0.25 \pm 0.11$
$(2.6, 4.0) \times 10^{-3}$	0.00328	$465 \pm 24 \pm 6 \pm 27$	$2.87 \pm 0.15 \pm 0.04 \pm 0.17 \pm 0.08$
$(4.0, 6.2) \times 10^{-3}$	0.00498	$229 \pm 14 \pm 3 \pm 14$	$1.48 \pm 0.09 \pm 0.02 \pm 0.09 \pm 0.04$
$(6.2, 12.1) \times 10^{-3}$	0.00833	$51 \pm 5 \pm 1 \pm 4$	$0.40 \pm 0.04 \pm 0.01 \pm 0.03 \pm 0.03$
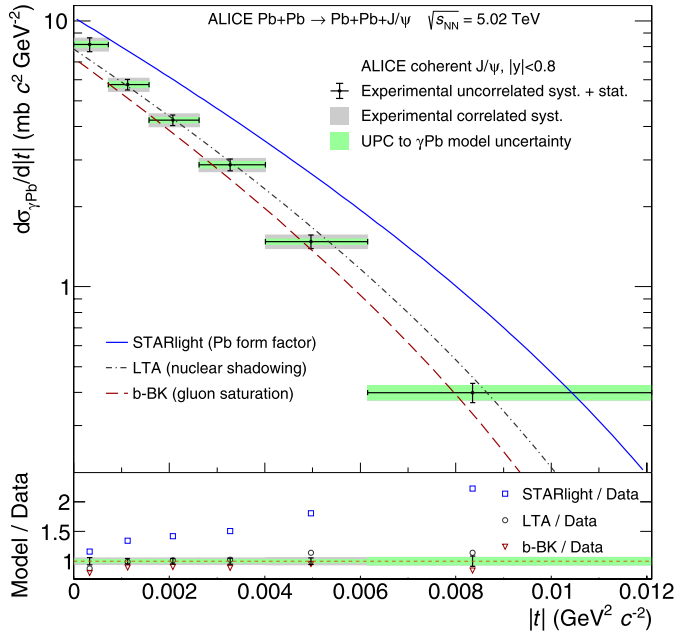
Fig. 2. Dependence on $|t|$ of the photonuclear cross section for the coherent photoproduction of J/ψ off Pb compared with model predictions [10,11,27] (top panel), where for LTA the *low shadowing* case is shown (see text). Model to data ratio for each prediction in each measured point (bottom panel). The uncertainties are split to those originating from experiment and to those originating from the correction to go from the UPC to the photonuclear cross section.

distribution, propagating the uncertainties of the f_I and f_D corrections, see Eq. (1), and the uncertainty related to the unfolding process. The uncorrelated systematic uncertainty from signal extraction and the quadratic sum of correlated systematic uncertainties are shown in Table 3.

The results for the photonuclear cross section are listed in Table 3 and shown in Fig. 2, where the measurement is compared with several theoretical predictions. The average $|t|$ ($\langle|t|\rangle$) quoted in Table 3 was estimated from the $|t|$-distribution used in the response matrix based on measured data (see above). The mean of the ensuing distribution in a given p_T^2 interval was taken to be $\langle|t|\rangle$.

STARlight utilises the vector meson dominance model and a parameterisation of the existing data on exclusive photoproduction of J/ψ off protons coupled with a Glauber-like formalism to obtain the photonuclear cross section. Since the $|t|$-dependence in this model comes from the Glauber calculation, meaning that it does not include explicitly gluon shadowing effects, it is an interesting baseline for comparisons (this approach is quite similar to the impulse approximation used in [41]). STARlight overestimates the measured cross section and the shape of the distribution appears to be wider than that of the measured data.

The LTA prediction by Guzey, Strikman and Zhalov [10] is based on the leading-twist approximation (LTA) of nuclear shadowing based on the combination of the Gribov–Glauber theory and inclusive diffractive data from HERA [42]. There are two LTA predictions; one called *high shadowing* and the other *low shadowing*. The low shadowing prediction is shown in Fig. 2. The shape obtained from this model is similar to that of the data and describes the cross section within experimental uncertainties. As shown in Fig. 3 of [10], the high-shadowing version of the model has a similar shape but the overall normalisation is smaller by factor around 1.7.

The b-BK model by Bendova et al. [11,43,44] is based on the colour dipole approach where the scattering amplitude is obtained from the impact-parameter dependent solution of the Balitsky–Kovchegov equation coupled to a nuclear-like initial condition [45,46] which incorporates saturation effects. This model also predicts the behaviour of the data quite well.

The different predictions of the STARlight and LTA or b-BK models reflect the effects of QCD dynamics (shadowing in LTA, saturation in b-BK) at small values of $x \sim 10^{-3}$ and highlight the importance of measuring the $|t|$-dependence of the photonuclear cross section.

5. Conclusions

The first measurement of the $|t|$-dependence of coherent J/ψ photonuclear production off Pb nuclei in UPCs is presented. The measurement was carried out with the ALICE detector at midrapidity, $|y| < 0.8$, in ultra-peripheral Pb–Pb collisions at $\sqrt{s_{NN}} = 5.02$ TeV and covers the small-x range $(0.3 - 1.4) \times 10^{-3}$. Photonuclear cross sections in six different intervals of $|t|$ are reported and compared with theoretical predictions. The measured cross section shows a $|t|$-dependent shape different from a model based on the Pb nuclear form factor and closer to the shape predicted by models including QCD dynamical effects in the form of shadowing (LTA) or saturation (b-BK). The difference in shape and magnitude between the LTA and b-BK models is of the same order as the current measurement uncertainties, but the large data sample expected in the LHC Run 3 [47] and the improvement in tracking from the upgrades of the ALICE detector [48] promise a much improved accuracy. These results highlight the importance of observables sensitive to the transverse gluonic structure of particles for extending the understanding of the high-energy limit of QCD.

Declaration of competing interest

The authors declare that they have no known competing financial interests or personal relationships that could have appeared to influence the work reported in this paper.

Acknowledgements

References

[1] C.A. Bertulani, S.R. Klein, J. Nystrand, Physics of ultra-peripheral nuclear collisions, Annu. Rev. Nucl. Part. Sci. 55 (2005) 271–310, arXiv:nucl-ex/0502005.

[2] A. Baltz, The physics of ultraperipheral collisions at the LHC, Phys. Rep. 458 (2008) 1–171, arXiv:0706.3356 [nucl-ex].

[3] J.G. Contreras, J.D. Tapia Takaki, Ultra-peripheral heavy-ion collisions at the LHC, Int. J. Mod. Phys. A 30 (2015) 1542012.

[4] S.R. Klein, H. Mäntysaari, Imaging the nucleus with high-energy photons, Nat. Rev. Phys. 1 (11) (2019) 662–674, arXiv:1910.10858 [hep-ex].

[5] V. Guzey, M. Strikman, M. Zhalov, Nucleon dissociation and incoherent J/ψ photoproduction on nuclei in ion ultraperipheral collisions at the Large Hadron Collider, Phys. Rev. C 99 (1) (2019) 015201, arXiv:1808.00740 [hep-ph].

[6] N. Armesto, Nuclear shadowing, J. Phys. G 32 (2006) R367–R394, arXiv:hep-ph/0604108.

[7] M. Ryskin, Diffractive J/ψ electroproduction in LLA QCD, Z. Phys. C 57 (1993) 89–92.

[8] V. Rebyakova, M. Strikman, M. Zhalov, Coherent ρ and J/ψ photoproduction in ultraperipheral processes with electromagnetic dissociation of heavy ions at RHIC and LHC, Phys. Lett. B 710 (2012) 647–653, arXiv:1109.0737 [hep-ph].

[9] J.L. Albacete, C. Marquet, Gluon saturation and initial conditions for relativistic heavy ion collisions, Prog. Part. Nucl. Phys. 76 (2014) 1–42, arXiv:1401.4866 [hep-ph].

[10] V. Guzey, M. Strikman, M. Zhalov, Accessing transverse nucleon and gluon distributions in heavy nuclei using coherent vector meson photoproduction at high energies in ion ultraperipheral collisions, Phys. Rev. C 95 (2) (2017) 025204, arXiv:1611.05471 [hep-ph].

[11] D. Bendova, J. Cepila, J.G. Contreras, M. Matas, Photonuclear J/ψ production at the LHC: proton-based versus nuclear dipole scattering amplitudes, arXiv:2006.12980 [hep-ph].

[12] ALICE Collaboration, B. Abelev, et al., Coherent J/ψ photoproduction in ultra-peripheral Pb-Pb collisions at $\sqrt{s_{NN}}$ = 2.76 TeV, Phys. Lett. B 718 (2013) 1273–1283, arXiv:1209.3715 [nucl-ex].

[13] ALICE Collaboration, E. Abbas, et al., Charmonium and e^+e^- pair photoproduction at mid-rapidity in ultra-peripheral Pb-Pb collisions at $\sqrt{s_{NN}}$ = 2.76 TeV, Eur. Phys. J. C 73 (11) (2013) 2617, arXiv:1305.1467 [nucl-ex].

[14] ALICE Collaboration, J. Adam, et al., Coherent ψ(2S) photo-production in ultra-peripheral Pb Pb collisions at $\sqrt{s_{NN}}$ = 2.76 TeV, Phys. Lett. B 751 (2015) 358–370, arXiv:1508.05076 [nucl-ex].

[15] ALICE Collaboration, S. Acharya, et al., Coherent J/ψ photoproduction at forward rapidity in ultra-peripheral Pb-Pb collisions at $\sqrt{s_{NN}}$ = 5.02 TeV, Phys. Lett. B 798 (2019) 134926, arXiv:1904.06272 [nucl-ex].

[16] CMS Collaboration, V. Khachatryan, et al., Coherent J/ψ photoproduction in ultra-peripheral PbPb collisions at $\sqrt{s_{NN}}$ = 2.76 TeV with the CMS experiment, Phys. Lett. B 772 (2017) 489–511, arXiv:1605.06966 [nucl-ex].

[17] J. Bartels, K.J. Golec-Biernat, K. Peters, On the dipole picture in the nonforward direction, Acta Phys. Pol. B 34 (2003) 3051–3068, arXiv:hep-ph/0301192.

[18] STAR Collaboration, L. Adamczyk, et al., Coherent diffractive photoproduction of ρ^0 mesons on gold nuclei at 200 GeV/nucleon-pair at the Relativistic Heavy Ion Collider, Phys. Rev. C 96 (5) (2017) 054904, arXiv:1702.07705 [nucl-ex].

[19] STAR Collaboration, J. Adam, et al., Observation of excess J/ψ yield at very low transverse momenta in Au+Au collisions at $\sqrt{s_{NN}}$ = 200 GeV and U+U collisions at $\sqrt{s_{NN}}$ = 193 GeV, Phys. Rev. Lett. 123 (13) (2019) 132302, arXiv:1904.11658 [hep-ex].

[20] ALICE Collaboration, K. Aamodt, et al., The ALICE experiment at the CERN LHC, J. Instrum. 3 (2008) S08002.

[21] ALICE Collaboration, B.B. Abelev, et al., Performance of the ALICE Experiment at the CERN LHC, Int. J. Mod. Phys. A 29 (2014) 1430044, arXiv:1402.4476 [nucl-ex].

[22] LHC Forward Physics Working Group Collaboration, K. Akiba, et al., LHC forward physics, J. Phys. G 43 (2016) 110201, arXiv:1611.05079 [hep-ph].

[23] M. Broz, et al., Performance of ALICE AD modules in the CERN PS test beam, arXiv:2006.14982 [physics.ins-det].

[24] ALICE Collaboration, ALICE luminosity determination for Pb–Pb, collisions at $\sqrt{s_{NN}}$ = 5.02 TeV, ALICE-PUBLIC-2021-001.

[25] M. Oreglia, A Study of the Reactions $\psi' \to \gamma\gamma\psi$, PhD thesis, Stanford University, 1980, https://www.slac.stanford.edu/cgi-bin/getdoc/slac-r-236.pdf, SLAC Report SLAC-R-236, Appendix D.

[26] H1 Collaboration, C. Alexa, et al., Elastic and proton-dissociative photoproduction of J/ψ mesons at HERA, Eur. Phys. J. C 73 (6) (2013) 2466, arXiv:1304.5162 [hep-ex].

[27] S.R. Klein, J. Nystrand, J. Seger, Y. Gorbunov, J. Butterworth, STARlight: a Monte Carlo simulation program for ultra-peripheral collisions of relativistic ions, Comput. Phys. Commun. 212 (2017) 258–268, arXiv:1607.03838 [hep-ph].

[28] R. Brun, F. Bruyant, F. Carminati, S. Giani, M. Maire, A. McPherson, G. Patrick, L. Urban, GEANT: detector description and simulation tool, Oct 1994, in: CERN Program Library, CERN, Geneva, 1993, http://cds.cern.ch/record/1082634, Long Writeup W5013.

[29] I. Pshenichnov, I. Mishustin, J. Bondorf, A. Botvina, A. Ilinov, Particle emission following Coulomb excitation in ultrarelativistic heavy ion collisions, Phys. Rev. C 60 (1999) 044901, arXiv:nucl-th/9901061.

[30] G. D'Agostini, A multidimensional unfolding method based on Bayes' theorem, Nucl. Instrum. Methods A 362 (1995) 487–498.

[31] A. Hocker, V. Kartvelishvili, SVD approach to data unfolding, Nucl. Instrum. Methods A 372 (1996) 469–481, arXiv:hep-ph/9509307.

[32] T. Adye, Unfolding algorithms and tests using RooUnfold, in: PHYSTAT 2011, CERN, Geneva, 2011, pp. 313–318, arXiv:1105.1160 [physics.data-an].

[33] Particle Data Group Collaboration, P.A. Zyla, et al., Review of particle physics, Prog. Theor. Exp. Phys. 2020 (2020), 083C01.

[34] S.R. Klein, J. Nystrand, Interference in exclusive vector meson production in heavy ion collisions, Phys. Rev. Lett. 84 (2000) 2330–2333, arXiv:hep-ph/9909237.

[35] STAR Collaboration, B. Abelev, et al., Observation of two-source interference in the photoproduction reaction $AuAu \to AuAu\rho^0$, Phys. Rev. Lett. 102 (2009) 112301, arXiv:0812.1063 [nucl-ex].

[36] W. Zha, S.R. Klein, R. Ma, L. Ruan, T. Todoroki, Z. Tang, Z. Xu, C. Yang, Q. Yang, S. Yang, Coherent J/ψ photoproduction in hadronic heavy-ion collisions, Phys. Rev. C 97 (4) (2018) 044910, arXiv:1705.01460 [nucl-th].

[37] J.G. Contreras, Gluon shadowing at small x from coherent J/ψ photoproduction data at energies available at the CERN Large Hadron Collider, Phys. Rev. C 96 (1) (2017) 015203, arXiv:1610.03350 [nucl-ex].

[38] M. Broz, J.G. Contreras, J.D. Tapia Takaki, A generator of forward neutrons for ultra-peripheral collisions: $n_O^o n$, Comput. Phys. Commun. 253 (2020) 107181, arXiv:1908.08263 [nucl-th].

[39] M. Vidovic, M. Greiner, C. Best, G. Soff, Impact parameter dependence of the electromagnetic particle production in ultrarelativistic heavy ion collisions, Phys. Rev. C 47 (1993) 2308–2319.

[40] K. Hencken, D. Trautmann, G. Baur, Photon-photon luminosities in relativistic heavy ion collisions at LHC energies, Z. Phys. C 68 (1995) 473–480, arXiv:nucl-th/9503004.

[41] V. Guzey, M. Zhalov, Exclusive J/ψ production in ultraperipheral collisions at the LHC: constrains on the gluon distributions in the proton and nuclei, J. High Energy Phys. 10 (2013) 207, arXiv:1307.4526 [hep-ph].

[42] L. Frankfurt, V. Guzey, M. Strikman, Leading twist nuclear shadowing phenomena in hard processes with nuclei, Phys. Rep. 512 (2012) 255–393, arXiv:1106.2091 [hep-ph].

[43] J. Cepila, J.G. Contreras, M. Matas, Collinearly improved kernel suppresses Coulomb tails in the impact-parameter dependent Balitsky–Kovchegov evolution, Phys. Rev. D 99 (5) (2019) 051502, arXiv:1812.02548 [hep-ph].

[44] D. Bendova, J. Cepila, J.G. Contreras, M. Matas, Solution to the Balitsky–Kovchegov equation with the collinearly improved kernel including impact-parameter dependence, Phys. Rev. D 100 (5) (2019) 054015, arXiv:1907.12123 [hep-ph].

[45] I. Balitsky, Operator expansion for high-energy scattering, Nucl. Phys. B 463 (1996) 99–160, arXiv:hep-ph/9509348 [hep-ph].

[46] Y.V. Kovchegov, Small-x F_2 structure function of a nucleus including multiple pomeron exchanges, Phys. Rev. D 60 (1999) 034008, arXiv:hep-ph/9901281 [hep-ph].

[47] Z. Citron, et al., Report from Working Group 5: future physics opportunities for high-density QCD at the LHC with heavy-ion and proton beams, CERN Yellow Rep. Monogr. 7 (2019) 1159–1410, arXiv:1812.06772 [hep-ph].

[48] ALICE Collaboration, B. Abelev, et al., Upgrade of the ALICE experiment: letter of intent, J. Phys. G 41 (2014) 087001.

ALICE Collaboration

S. Acharya [142], D. Adamová [97], A. Adler [75], J. Adolfsson [82], G. Aglieri Rinella [35], M. Agnello [31], N. Agrawal [55], Z. Ahammed [142], S. Ahmad [16], S.U. Ahn [77], Z. Akbar [52], A. Akindinov [94], M. Al-Turany [109], D.S.D. Albuquerque [124], D. Aleksandrov [90], B. Alessandro [60], H.M. Alfanda [7], R. Alfaro Molina [72], B. Ali [16], Y. Ali [14], A. Alici [26], N. Alizadehvandchali [127], A. Alkin [35], J. Alme [21], T. Alt [69], L. Altenkamper [21], I. Altsybeev [115], M.N. Anaam [7], C. Andrei [49], D. Andreou [92], A. Andronic [145], V. Anguelov [106], T. Antičić [110], F. Antinori [58], P. Antonioli [55], C. Anuj [16], N. Apadula [81], L. Aphecetche [117], H. Appelshäuser [69], S. Arcelli [26], R. Arnaldi [60], M. Arratia [81], I.C. Arsene [20], M. Arslandok [147,106], A. Augustinus [35], R. Averbeck [109], S. Aziz [79], M.D. Azmi [16], A. Badalà [57], Y.W. Baek [42], X. Bai [109], R. Bailhache [69], R. Bala [103], A. Balbino [31], A. Baldisseri [139], M. Ball [44], D. Banerjee [4], R. Barbera [27], L. Barioglio [25], M. Barlou [86], G.G. Barnaföldi [146], L.S. Barnby [96], V. Barret [136], C. Bartels [129], K. Barth [35], E. Bartsch [69], F. Baruffaldi [28], N. Bastid [136], S. Basu [82,144], G. Batigne [117], B. Batyunya [76], D. Bauri [50], J.L. Bazo Alba [114], I.G. Bearden [91], C. Beattie [147], I. Belikov [138], A.D.C. Bell Hechavarria [145], F. Bellini [35], R. Bellwied [127], S. Belokurova [115], V. Belyaev [95], G. Bencedi [70,146], S. Beole [25], A. Bercuci [49], Y. Berdnikov [100], A. Berdnikova [106], D. Berenyi [146], L. Bergmann [106], M.G. Besoiu [68], L. Betev [35], P.P. Bhaduri [142], A. Bhasin [103], I.R. Bhat [103], M.A. Bhat [4], B. Bhattacharjee [43], P. Bhattacharya [23], A. Bianchi [25], L. Bianchi [25], N. Bianchi [53], J. Bielčík [38], J. Bielčíková [97], A. Bilandzic [107], G. Biro [146], S. Biswas [4], J.T. Blair [121], D. Blau [90], M.B. Blidaru [109], C. Blume [69], G. Boca [29], F. Bock [98], A. Bogdanov [95], S. Boi [23], J. Bok [62], L. Boldizsár [146], A. Bolozdynya [95], M. Bombara [39], P.M. Bond [35], G. Bonomi [141], H. Borel [139], A. Borissov [83,95], H. Bossi [147], E. Botta [25], L. Bratrud [69], P. Braun-Munzinger [109], M. Bregant [123], M. Broz [38], G.E. Bruno [108,34], M.D. Buckland [129], D. Budnikov [111], H. Buesching [69], S. Bufalino [31], O. Bugnon [117], P. Buhler [116], P. Buncic [35], Z. Buthelezi [73,133], J.B. Butt [14], S.A. Bysiak [120], M. Cai [28,7], D. Caffarri [92], A. Caliva [109], E. Calvo Villar [114], J.M.M. Camacho [122], R.S. Camacho [46], P. Camerini [24], F.D.M. Canedo [123], A.A. Capon [116], F. Carnesecchi [26], R. Caron [139], J. Castillo Castellanos [139], E.A.R. Casula [23], F. Catalano [31], C. Ceballos Sanchez [76], P. Chakraborty [50], S. Chandra [142], W. Chang [7], S. Chapeland [35], M. Chartier [129], S. Chattopadhyay [142], S. Chattopadhyay [112], A. Chauvin [23], T.G. Chavez [46], C. Cheshkov [137], B. Cheynis [137], V. Chibante Barroso [35], D.D. Chinellato [124], S. Cho [62], P. Chochula [35], P. Christakoglou [92], C.H. Christensen [91], P. Christiansen [82], T. Chujo [135], C. Cicalo [56], L. Cifarelli [26], F. Cindolo [55], M.R. Ciupek [109], G. Clai [55,II], J. Cleymans [126],

F. Colamaria [54], J.S. Colburn [113], D. Colella [54,146], A. Collu [81], M. Colocci [35,26], M. Concas [60,III],
G. Conesa Balbastre [80], Z. Conesa del Valle [79], G. Contin [24], J.G. Contreras [38], T.M. Cormier [98], P. Cortese [32],
M.R. Cosentino [125], F. Costa [35], S. Costanza [29], P. Crochet [136], E. Cuautle [70], P. Cui [7], L. Cunqueiro [98],
A. Dainese [58], F.P.A. Damas [117,139], M.C. Danisch [106], A. Danu [68], I. Das [112], P. Das [88], P. Das [4], S. Das [4],
S. Dash [50], S. De [88], A. De Caro [30], G. de Cataldo [54], L. De Cilladi [25], J. de Cuveland [40], A. De Falco [23],
D. De Gruttola [30], N. De Marco [60], C. De Martin [24], S. De Pasquale [30], S. Deb [51], H.F. Degenhardt [123],
K.R. Deja [143], L. Dello Stritto [30], S. Delsanto [25], W. Deng [7], P. Dhankher [19], D. Di Bari [34], A. Di Mauro [35],
R.A. Diaz [8], T. Dietel [126], Y. Ding [7], R. Divià [35], D.U. Dixit [19], Ø. Djuvsland [21], U. Dmitrieva [64], J. Do [62],
A. Dobrin [68], B. Dönigus [69], O. Dordic [20], A.K. Dubey [142], A. Dubla [109,92], S. Dudi [102], M. Dukhishyam [88],
P. Dupieux [136], T.M. Eder [145], R.J. Ehlers [98], V.N. Eikeland [21], D. Elia [54], B. Erazmus [117], F. Ercolessi [26],
F. Erhardt [101], A. Erokhin [115], M.R. Ersdal [21], B. Espagnon [79], G. Eulisse [35], D. Evans [113], S. Evdokimov [93],
L. Fabbietti [107], M. Faggin [28], J. Faivre [80], F. Fan [7], A. Fantoni [53], M. Fasel [98], P. Fecchio [31], A. Feliciello [60],
G. Feofilov [115], A. Fernández Téllez [46], A. Ferrero [139], A. Ferretti [25], A. Festanti [35], V.J.G. Feuillard [106],
J. Figiel [120], S. Filchagin [111], D. Finogeev [64], F.M. Fionda [21], G. Fiorenza [54], F. Flor [127], A.N. Flores [121],
S. Foertsch [73], P. Foka [109], S. Fokin [90], E. Fragiacomo [61], U. Fuchs [35], N. Funicello [30], C. Furget [80], A. Furs [64],
M. Fusco Girard [30], J.J. Gaardhøje [91], M. Gagliardi [25], A.M. Gago [114], A. Gal [138], C.D. Galvan [122], P. Ganoti [86],
C. Garabatos [109], J.R.A. Garcia [46], E. Garcia-Solis [10], K. Garg [117], C. Gargiulo [35], A. Garibli [89], K. Garner [145],
P. Gasik [107], E.F. Gauger [121], M.B. Gay Ducati [71], M. Germain [117], J. Ghosh [112], P. Ghosh [142], S.K. Ghosh [4],
M. Giacalone [26], P. Gianotti [53], P. Giubellino [109,60], P. Giubilato [28], A.M.C. Glaenzer [139], P. Glässel [106],
V. Gonzalez [144], L.H. González-Trueba [72], S. Gorbunov [40], L. Görlich [120], S. Gotovac [36], V. Grabski [72],
L.K. Graczykowski [143], K.L. Graham [113], L. Greiner [81], A. Grelli [63], C. Grigoras [35], V. Grigoriev [95],
A. Grigoryan [1,I], S. Grigoryan [76,1], O.S. Groettvik [21], F. Grosa [60], J.F. Grosse-Oetringhaus [35], R. Grosso [109],
R. Guernane [80], M. Guilbaud [117], M. Guittiere [117], K. Gulbrandsen [91], T. Gunji [134], A. Gupta [103],
R. Gupta [103], I.B. Guzman [46], R. Haake [147], M.K. Habib [109], C. Hadjidakis [79], H. Hamagaki [84], G. Hamar [146],
M. Hamid [7], R. Hannigan [121], M.R. Haque [143,88], A. Harlenderova [109], J.W. Harris [147], A. Harton [10],
J.A. Hasenbichler [35], H. Hassan [98], D. Hatzifotiadou [55], P. Hauer [44], L.B. Havener [147], S. Hayashi [134],
S.T. Heckel [107], E. Hellbär [69], H. Helstrup [37], T. Herman [38], E.G. Hernandez [46], G. Herrera Corral [9],
F. Herrmann [145], K.F. Hetland [37], H. Hillemanns [35], C. Hills [129], B. Hippolyte [138], B. Hohlweger [107],
J. Honermann [145], G.H. Hong [148], D. Horak [38], S. Hornung [109], R. Hosokawa [15], P. Hristov [35], C. Huang [79],
C. Hughes [132], P. Huhn [69], T.J. Humanic [99], H. Hushnud [112], L.A. Husova [145], N. Hussain [43], D. Hutter [40],
J.P. Iddon [35,129], R. Ilkaev [111], H. Ilyas [14], M. Inaba [135], G.M. Innocenti [35], M. Ippolitov [90], A. Isakov [38,97],
M.S. Islam [112], M. Ivanov [109], V. Ivanov [100], V. Izucheev [93], B. Jacak [81], N. Jacazio [35,55], P.M. Jacobs [81],
S. Jadlovska [119], J. Jadlovsky [119], S. Jaelani [63], C. Jahnke [123], M.J. Jakubowska [143], M.A. Janik [143],
T. Janson [75], M. Jercic [101], O. Jevons [113], M. Jin [127], F. Jonas [98,145], P.G. Jones [113], J. Jung [69], M. Jung [69],
A. Junique [35], A. Jusko [113], P. Kalinak [65], A. Kalweit [35], V. Kaplin [95], S. Kar [7], A. Karasu Uysal [78],
D. Karatovic [101], O. Karavichev [64], T. Karavicheva [64], P. Karczmarczyk [143], E. Karpechev [64], A. Kazantsev [90],
U. Kebschull [75], R. Keidel [48], M. Keil [35], B. Ketzer [44], Z. Khabanova [92], A.M. Khan [7], S. Khan [16],
A. Khanzadeev [100], Y. Kharlov [93], A. Khatun [16], A. Khuntia [120], B. Kileng [37], B. Kim [62], D. Kim [148],
D.J. Kim [128], E.J. Kim [74], H. Kim [17], J. Kim [148], J.S. Kim [42], J. Kim [106], J. Kim [148], J. Kim [74], M. Kim [106],
S. Kim [18], T. Kim [148], S. Kirsch [69], I. Kisel [40], S. Kiselev [94], A. Kisiel [143], J.L. Klay [6], J. Klein [35,60], S. Klein [81],
C. Klein-Bösing [145], M. Kleiner [69], T. Klemenz [107], A. Kluge [35], A.G. Knospe [127], C. Kobdaj [118],
M.K. Köhler [106], T. Kollegger [109], A. Kondratyev [76], N. Kondratyeva [95], E. Kondratyuk [93], J. Konig [69],
S.A. Konigstorfer [107], P.J. Konopka [2,35], G. Kornakov [143], S.D. Koryciak [2], L. Koska [119], O. Kovalenko [87],
V. Kovalenko [115], M. Kowalski [120], I. Králik [65], A. Kravčáková [39], L. Kreis [109], M. Krivda [113,65], F. Krizek [97],
K. Krizkova Gajdosova [38], M. Kroesen [106], M. Krüger [69], E. Kryshen [100], M. Krzewicki [40], V. Kučera [35],
C. Kuhn [138], P.G. Kuijer [92], T. Kumaoka [135], L. Kumar [102], S. Kundu [88], P. Kurashvili [87], A. Kurepin [64],
A.B. Kurepin [64], A. Kuryakin [111], S. Kushpil [97], J. Kvapil [113], M.J. Kweon [62], J.Y. Kwon [62], Y. Kwon [148],
S.L. La Pointe [40], P. La Rocca [27], Y.S. Lai [81], A. Lakrathok [118], M. Lamanna [35], R. Langoy [131], K. Lapidus [35],
P. Larionov [53], E. Laudi [35], L. Lautner [35], R. Lavicka [38], T. Lazareva [115], R. Lea [24], J. Lee [135], J. Lehrbach [40],
R.C. Lemmon [96], I. León Monzón [122], E.D. Lesser [19], M. Lettrich [35], P. Lévai [146], X. Li [11], X.L. Li [7], J. Lien [131],
R. Lietava [113], B. Lim [17], S.H. Lim [17], V. Lindenstruth [40], A. Lindner [49], C. Lippmann [109], A. Liu [19], J. Liu [129],
I.M. Lofnes [21], V. Loginov [95], C. Loizides [98], P. Loncar [36], J.A. Lopez [106], X. Lopez [136], E. López Torres [8],
J.R. Luhder [145], M. Lunardon [28], G. Luparello [61], Y.G. Ma [41], A. Maevskaya [64], M. Mager [35],

S.M. Mahmood [20], T. Mahmoud [44], A. Maire [138], R.D. Majka [147,I], M. Malaev [100], Q.W. Malik [20], L. Malinina [76,IV], D. Mal'Kevich [94], N. Mallick [51], P. Malzacher [109], G. Mandaglio [33,57], V. Manko [90], F. Manso [136], V. Manzari [54], Y. Mao [7], J. Mareš [67], G.V. Margagliotti [24], A. Margotti [55], A. Marín [109], C. Markert [121], M. Marquard [69], N.A. Martin [106], P. Martinengo [35], J.L. Martinez [127], M.I. Martínez [46], G. Martínez García [117], S. Masciocchi [109], M. Masera [25], A. Masoni [56], L. Massacrier [79], A. Mastroserio [140,54], A.M. Mathis [107], O. Matonoha [82], P.F.T. Matuoka [123], A. Matyja [120], C. Mayer [120], A.L. Mazuecos [35], F. Mazzaschi [25], M. Mazzilli [35,54], M.A. Mazzoni [59], A.F. Mechler [69], F. Meddi [22], Y. Melikyan [64], A. Menchaca-Rocha [72], E. Meninno [116,30], A.S. Menon [127], M. Meres [13], S. Mhlanga [126], Y. Miake [135], L. Micheletti [25], L.C. Migliorin [137], D.L. Mihaylov [107], K. Mikhaylov [76,94], A.N. Mishra [146,70], D. Miśkowiec [109], A. Modak [4], N. Mohammadi [35], A.P. Mohanty [63], B. Mohanty [88], M. Mohisin Khan [16], Z. Moravcova [91], C. Mordasini [107], D.A. Moreira De Godoy [145], L.A.P. Moreno [46], I. Morozov [64], A. Morsch [35], T. Mrnjavac [35], V. Muccifora [53], E. Mudnic [36], D. Mühlheim [145], S. Muhuri [142], J.D. Mulligan [81], A. Mulliri [23], M.G. Munhoz [123], R.H. Munzer [69], H. Murakami [134], S. Murray [126], L. Musa [35], J. Musinsky [65], C.J. Myers [127], J.W. Myrcha [143], B. Naik [50], R. Nair [87], B.K. Nandi [50], R. Nania [55], E. Nappi [54], M.U. Naru [14], A.F. Nassirpour [82], C. Nattrass [132], S. Nazarenko [111], A. Neagu [20], L. Nellen [70], S.V. Nesbo [37], G. Neskovic [40], D. Nesterov [115], B.S. Nielsen [91], S. Nikolaev [90], S. Nikulin [90], V. Nikulin [100], F. Noferini [55], S. Noh [12], P. Nomokonov [76], J. Norman [129], N. Novitzky [135], P. Nowakowski [143], A. Nyanin [90], J. Nystrand [21], M. Ogino [84], A. Ohlson [82], J. Oleniacz [143], A.C. Oliveira Da Silva [132], M.H. Oliver [147], A. Onnerstad [128], C. Oppedisano [60], A. Ortiz Velasquez [70], T. Osako [47], A. Oskarsson [82], J. Otwinowski [120], K. Oyama [84], Y. Pachmayer [106], S. Padhan [50], D. Pagano [141], G. Paić [70], A. Palasciano [54], J. Pan [144], S. Panebianco [139], P. Pareek [142], J. Park [62], J.E. Parkkila [128], S. Parmar [102], S.P. Pathak [127], B. Paul [23], J. Pazzini [141], H. Pei [7], T. Peitzmann [63], X. Peng [7], L.G. Pereira [71], H. Pereira Da Costa [139], D. Peresunko [90], G.M. Perez [8], S. Perrin [139], Y. Pestov [5], V. Petráček [38], M. Petrovici [49], R.P. Pezzi [71], S. Piano [61], M. Pikna [13], P. Pillot [117], O. Pinazza [55,35], L. Pinsky [127], C. Pinto [27], S. Pisano [53], M. Płoskoń [81], M. Planinic [101], F. Pliquett [69], M.G. Poghosyan [98], B. Polichtchouk [93], N. Poljak [101], A. Pop [49], S. Porteboeuf-Houssais [136], J. Porter [81], V. Pozdniakov [76], S.K. Prasad [4], R. Preghenella [55], F. Prino [60], C.A. Pruneau [144], I. Pshenichnov [64], M. Puccio [35], S. Qiu [92], L. Quaglia [25], R.E. Quishpe [127], S. Ragoni [113], A. Rakotozafindrabe [139], L. Ramello [32], F. Rami [138], S.A.R. Ramirez [46], A.G.T. Ramos [34], R. Raniwala [104], S. Raniwala [104], S.S. Räsänen [45], R. Rath [51], I. Ravasenga [92], K.F. Read [98,132], A.R. Redelbach [40], K. Redlich [87,V], A. Rehman [21], P. Reichelt [69], F. Reidt [35], R. Renfordt [69], Z. Rescakova [39], K. Reygers [106], A. Riabov [100], V. Riabov [100], T. Richert [82,91], M. Richter [20], P. Riedler [35], W. Riegler [35], F. Riggi [27], C. Ristea [68], S.P. Rode [51], M. Rodríguez Cahuantzi [46], K. Røed [20], R. Rogalev [93], E. Rogochaya [76], T.S. Rogoschinski [69], D. Rohr [35], D. Röhrich [21], P.F. Rojas [46], P.S. Rokita [143], F. Ronchetti [53], A. Rosano [33,57], E.D. Rosas [70], A. Rossi [58], A. Rotondi [29], A. Roy [51], P. Roy [112], N. Rubini [26], O.V. Rueda [82], R. Rui [24], B. Rumyantsev [76], A. Rustamov [89], E. Ryabinkin [90], Y. Ryabov [100], A. Rybicki [120], H. Rytkonen [128], W. Rzesa [143], O.A.M. Saarimaki [45], R. Sadek [117], S. Sadovsky [93], J. Saetre [21], K. Šafařík [38], S.K. Saha [142], S. Saha [88], B. Sahoo [50], P. Sahoo [50], R. Sahoo [51], S. Sahoo [66], D. Sahu [51], P.K. Sahu [66], J. Saini [142], S. Sakai [135], S. Sambyal [103], V. Samsonov [100,95,I], D. Sarkar [144], N. Sarkar [142], P. Sarma [43], V.M. Sarti [107], M.H.P. Sas [147,63], J. Schambach [98,121], H.S. Scheid [69], C. Schiaua [49], R. Schicker [106], A. Schmah [106], C. Schmidt [109], H.R. Schmidt [105], M.O. Schmidt [106], M. Schmidt [105], N.V. Schmidt [98,69], A.R. Schmier [132], R. Schotter [138], J. Schukraft [35], Y. Schutz [138], K. Schwarz [109], K. Schweda [109], G. Scioli [26], E. Scomparin [60], J.E. Seger [15], Y. Sekiguchi [134], D. Sekihata [134], I. Selyuzhenkov [109,95], S. Senyukov [138], J.J. Seo [62], D. Serebryakov [64], L. Šerkšnytė [107], A. Sevcenco [68], A. Shabanov [64], A. Shabetai [117], R. Shahoyan [35], W. Shaikh [112], A. Shangaraev [93], A. Sharma [102], H. Sharma [120], M. Sharma [103], N. Sharma [102], S. Sharma [103], O. Sheibani [127], A.I. Sheikh [142], K. Shigaki [47], M. Shimomura [85], S. Shirinkin [94], Q. Shou [41], Y. Sibiriak [90], S. Siddhanta [56], T. Siemiarczuk [87], T.F. Silva [123], D. Silvermyr [82], G. Simatovic [92], G. Simonetti [35], B. Singh [107], R. Singh [88], R. Singh [103], R. Singh [51], V.K. Singh [142], V. Singhal [142], T. Sinha [112], B. Sitar [13], M. Sitta [32], T.B. Skaali [20], G. Skorodumovs [106], M. Slupecki [45], N. Smirnov [147], R.J.M. Snellings [63], C. Soncco [114], J. Song [127], A. Songmoolnak [118], F. Soramel [28], S. Sorensen [132], I. Sputowska [120], J. Stachel [106], I. Stan [68], P.J. Steffanic [132], S.F. Stiefelmaier [106], D. Stocco [117], M.M. Storetvedt [37], C.P. Stylianidis [92], A.A.P. Suaide [123], T. Sugitate [47], C. Suire [79], M. Suljic [35], R. Sultanov [94], M. Šumbera [97], V. Sumberia [103], S. Sumowidagdo [52], S. Swain [66], A. Szabo [13], I. Szarka [13], U. Tabassam [14], S.F. Taghavi [107], G. Taillepied [136], J. Takahashi [124], G.J. Tambave [21], S. Tang [136,7], Z. Tang [130],

M. Tarhini [117], M.G. Tarzila [49], A. Tauro [35], G. Tejeda Muñoz [46], A. Telesca [35], L. Terlizzi [25], C. Terrevoli [127], G. Tersimonov [3], S. Thakur [142], D. Thomas [121], R. Tieulent [137], A. Tikhonov [64], A.R. Timmins [127], M. Tkacik [119], A. Toia [69], N. Topilskaya [64], M. Toppi [53], F. Torales-Acosta [19], S.R. Torres [38], A. Trifiró [33,57], S. Tripathy [70], T. Tripathy [50], S. Trogolo [28], G. Trombetta [34], V. Trubnikov [3], W.H. Trzaska [128], T.P. Trzcinski [143], B.A. Trzeciak [38], A. Tumkin [111], R. Turrisi [58], T.S. Tveter [20], K. Ullaland [21], E.N. Umaka [127], A. Uras [137], M. Urioni [141], G.L. Usai [23], M. Vala [39], N. Valle [29], S. Vallero [60], N. van der Kolk [63], L.V.R. van Doremalen [63], M. van Leeuwen [92], P. Vande Vyvre [35], D. Varga [146], Z. Varga [146], M. Varga-Kofarago [146], A. Vargas [46], M. Vasileiou [86], A. Vasiliev [90], O. Vázquez Doce [107], V. Vechernin [115], E. Vercellin [25], S. Vergara Limón [46], L. Vermunt [63], R. Vértesi [146], M. Verweij [63], L. Vickovic [36], Z. Vilakazi [133], O. Villalobos Baillie [113], G. Vino [54], A. Vinogradov [90], T. Virgili [30], V. Vislavicius [91], A. Vodopyanov [76], B. Volkel [35], M.A. Völkl [105], K. Voloshin [94], S.A. Voloshin [144], G. Volpe [34], B. von Haller [35], I. Vorobyev [107], D. Voscek [119], J. Vrláková [39], B. Wagner [21], M. Weber [116], A. Wegrzynek [35], S.C. Wenzel [35], J.P. Wessels [145], J. Wiechula [69], J. Wikne [20], G. Wilk [87], J. Wilkinson [109], G.A. Willems [145], E. Willsher [113], B. Windelband [106], M. Winn [139], W.E. Witt [132], J.R. Wright [121], Y. Wu [130], R. Xu [7], S. Yalcin [78], Y. Yamaguchi [47], K. Yamakawa [47], S. Yang [21], S. Yano [47,139], Z. Yin [7], H. Yokoyama [63], I.-K. Yoo [17], J.H. Yoon [62], S. Yuan [21], A. Yuncu [106], V. Yurchenko [3], V. Zaccolo [24], A. Zaman [14], C. Zampolli [35], H.J.C. Zanoli [63], N. Zardoshti [35], A. Zarochentsev [115], P. Závada [67], N. Zaviyalov [111], H. Zbroszczyk [143], M. Zhalov [100], S. Zhang [41], X. Zhang [7], Y. Zhang [130], V. Zherebchevskii [115], Y. Zhi [11], D. Zhou [7], Y. Zhou [91], J. Zhu [7,109], Y. Zhu [7], A. Zichichi [26], G. Zinovjev [3], N. Zurlo [141]

[1] *A.I. Alikhanyan National Science Laboratory (Yerevan Physics Institute) Foundation, Yerevan, Armenia*
[2] *AGH University of Science and Technology, Cracow, Poland*
[3] *Bogolyubov Institute for Theoretical Physics, National Academy of Sciences of Ukraine, Kiev, Ukraine*
[4] *Bose Institute, Department of Physics and Centre for Astroparticle Physics and Space Science (CAPSS), Kolkata, India*
[5] *Budker Institute for Nuclear Physics, Novosibirsk, Russia*
[6] *California Polytechnic State University, San Luis Obispo, CA, United States*
[7] *Central China Normal University, Wuhan, China*
[8] *Centro de Aplicaciones Tecnológicas y Desarrollo Nuclear (CEADEN), Havana, Cuba*
[9] *Centro de Investigación y de Estudios Avanzados (CINVESTAV), Mexico City and Mérida, Mexico*
[10] *Chicago State University, Chicago, IL, United States*
[11] *China Institute of Atomic Energy, Beijing, China*
[12] *Chungbuk National University, Cheongju, Republic of Korea*
[13] *Comenius University Bratislava, Faculty of Mathematics, Physics and Informatics, Bratislava, Slovakia*
[14] *COMSATS University Islamabad, Islamabad, Pakistan*
[15] *Creighton University, Omaha, NE, United States*
[16] *Department of Physics, Aligarh Muslim University, Aligarh, India*
[17] *Department of Physics, Pusan National University, Pusan, Republic of Korea*
[18] *Department of Physics, Sejong University, Seoul, Republic of Korea*
[19] *Department of Physics, University of California, Berkeley, CA, United States*
[20] *Department of Physics, University of Oslo, Oslo, Norway*
[21] *Department of Physics and Technology, University of Bergen, Bergen, Norway*
[22] *Dipartimento di Fisica dell'Università 'La Sapienza' and Sezione INFN, Rome, Italy*
[23] *Dipartimento di Fisica dell'Università and Sezione INFN, Cagliari, Italy*
[24] *Dipartimento di Fisica dell'Università and Sezione INFN, Trieste, Italy*
[25] *Dipartimento di Fisica dell'Università and Sezione INFN, Turin, Italy*
[26] *Dipartimento di Fisica e Astronomia dell'Università and Sezione INFN, Bologna, Italy*
[27] *Dipartimento di Fisica e Astronomia dell'Università and Sezione INFN, Catania, Italy*
[28] *Dipartimento di Fisica e Astronomia dell'Università and Sezione INFN, Padova, Italy*
[29] *Dipartimento di Fisica e Nucleare e Teorica, Università di Pavia and Sezione INFN, Pavia, Italy*
[30] *Dipartimento di Fisica 'E.R. Caianiello' dell'Università and Gruppo Collegato INFN, Salerno, Italy*
[31] *Dipartimento DISAT del Politecnico and Sezione INFN, Turin, Italy*
[32] *Dipartimento di Scienze e Innovazione Tecnologica dell'Università del Piemonte Orientale and INFN Sezione di Torino, Alessandria, Italy*
[33] *Dipartimento di Scienze MIFT, Università di Messina, Messina, Italy*
[34] *Dipartimento Interateneo di Fisica 'M. Merlin' and Sezione INFN, Bari, Italy*
[35] *European Organization for Nuclear Research (CERN), Geneva, Switzerland*
[36] *Faculty of Electrical Engineering, Mechanical Engineering and Naval Architecture, University of Split, Split, Croatia*
[37] *Faculty of Engineering and Science, Western Norway University of Applied Sciences, Bergen, Norway*
[38] *Faculty of Nuclear Sciences and Physical Engineering, Czech Technical University in Prague, Prague, Czech Republic*
[39] *Faculty of Science, P.J. Šafárik University, Košice, Slovakia*
[40] *Frankfurt Institute for Advanced Studies, Johann Wolfgang Goethe-Universität Frankfurt, Frankfurt, Germany*
[41] *Fudan University, Shanghai, China*
[42] *Gangneung-Wonju National University, Gangneung, Republic of Korea*
[43] *Gauhati University, Department of Physics, Guwahati, India*
[44] *Helmholtz-Institut für Strahlen- und Kernphysik, Rheinische Friedrich-Wilhelms-Universität Bonn, Bonn, Germany*
[45] *Helsinki Institute of Physics (HIP), Helsinki, Finland*
[46] *High Energy Physics Group, Universidad Autónoma de Puebla, Puebla, Mexico*
[47] *Hiroshima University, Hiroshima, Japan*
[48] *Hochschule Worms, Zentrum für Technologietransfer und Telekommunikation (ZTT), Worms, Germany*
[49] *Horia Hulubei National Institute of Physics and Nuclear Engineering, Bucharest, Romania*
[50] *Indian Institute of Technology Bombay (IIT), Mumbai, India*
[51] *Indian Institute of Technology Indore, Indore, India*

52 Indonesian Institute of Sciences, Jakarta, Indonesia
53 INFN, Laboratori Nazionali di Frascati, Frascati, Italy
54 INFN, Sezione di Bari, Bari, Italy
55 INFN, Sezione di Bologna, Bologna, Italy
56 INFN, Sezione di Cagliari, Cagliari, Italy
57 INFN, Sezione di Catania, Catania, Italy
58 INFN, Sezione di Padova, Padova, Italy
59 INFN, Sezione di Roma, Rome, Italy
60 INFN, Sezione di Torino, Turin, Italy
61 INFN, Sezione di Trieste, Trieste, Italy
62 Inha University, Incheon, Republic of Korea
63 Institute for Gravitational and Subatomic Physics (GRASP), Utrecht University/Nikhef, Utrecht, Netherlands
64 Institute for Nuclear Research, Academy of Sciences, Moscow, Russia
65 Institute of Experimental Physics, Slovak Academy of Sciences, Košice, Slovakia
66 Institute of Physics, Homi Bhabha National Institute, Bhubaneswar, India
67 Institute of Physics of the Czech Academy of Sciences, Prague, Czech Republic
68 Institute of Space Science (ISS), Bucharest, Romania
69 Institut für Kernphysik, Johann Wolfgang Goethe-Universität Frankfurt, Frankfurt, Germany
70 Instituto de Ciencias Nucleares, Universidad Nacional Autónoma de México, Mexico City, Mexico
71 Instituto de Física, Universidade Federal do Rio Grande do Sul (UFRGS), Porto Alegre, Brazil
72 Instituto de Física, Universidad Nacional Autónoma de México, Mexico City, Mexico
73 iThemba LABS, National Research Foundation, Somerset West, South Africa
74 Jeonbuk National University, Jeonju, Republic of Korea
75 Johann-Wolfgang-Goethe Universität Frankfurt Institut für Informatik, Fachbereich Informatik und Mathematik, Frankfurt, Germany
76 Joint Institute for Nuclear Research (JINR), Dubna, Russia
77 Korea Institute of Science and Technology Information, Daejeon, Republic of Korea
78 KTO Karatay University, Konya, Turkey
79 Laboratoire de Physique des 2 Infinis, Irène Joliot-Curie, Orsay, France
80 Laboratoire de Physique Subatomique et de Cosmologie, Université Grenoble-Alpes, CNRS-IN2P3, Grenoble, France
81 Lawrence Berkeley National Laboratory, Berkeley, CA, United States
82 Lund University Department of Physics, Division of Particle Physics, Lund, Sweden
83 Moscow Institute for Physics and Technology, Moscow, Russia
84 Nagasaki Institute of Applied Science, Nagasaki, Japan
85 Nara Women's University (NWU), Nara, Japan
86 National and Kapodistrian University of Athens, School of Science, Department of Physics, Athens, Greece
87 National Centre for Nuclear Research, Warsaw, Poland
88 National Institute of Science Education and Research, Homi Bhabha National Institute, Jatni, India
89 National Nuclear Research Center, Baku, Azerbaijan
90 National Research Centre Kurchatov Institute, Moscow, Russia
91 Niels Bohr Institute, University of Copenhagen, Copenhagen, Denmark
92 Nikhef, National institute for subatomic physics, Amsterdam, Netherlands
93 NRC Kurchatov Institute IHEP, Protvino, Russia
94 NRC "Kurchatov" Institute – ITEP, Moscow, Russia
95 NRNU Moscow Engineering Physics Institute, Moscow, Russia
96 Nuclear Physics Group, STFC Daresbury Laboratory, Daresbury, United Kingdom
97 Nuclear Physics Institute of the Czech Academy of Sciences, Řež u Prahy, Czech Republic
98 Oak Ridge National Laboratory, Oak Ridge, TN, United States
99 Ohio State University, Columbus, OH, United States
100 Petersburg Nuclear Physics Institute, Gatchina, Russia
101 Physics department, Faculty of science, University of Zagreb, Zagreb, Croatia
102 Physics Department, Panjab University, Chandigarh, India
103 Physics Department, University of Jammu, Jammu, India
104 Physics Department, University of Rajasthan, Jaipur, India
105 Physikalisches Institut, Eberhard-Karls-Universität Tübingen, Tübingen, Germany
106 Physikalisches Institut, Ruprecht-Karls-Universität Heidelberg, Heidelberg, Germany
107 Physik Department, Technische Universität München, Munich, Germany
108 Politecnico di Bari and Sezione INFN, Bari, Italy
109 Research Division and ExtreMe Matter Institute EMMI, GSI Helmholtzzentrum für Schwerionenforschung GmbH, Darmstadt, Germany
110 Rudjer Bošković Institute, Zagreb, Croatia
111 Russian Federal Nuclear Center (VNIIEF), Sarov, Russia
112 Saha Institute of Nuclear Physics, Homi Bhabha National Institute, Kolkata, India
113 School of Physics and Astronomy, University of Birmingham, Birmingham, United Kingdom
114 Sección Física, Departamento de Ciencias, Pontificia Universidad Católica del Perú, Lima, Peru
115 St. Petersburg State University, St. Petersburg, Russia
116 Stefan Meyer Institut für Subatomare Physik (SMI), Vienna, Austria
117 SUBATECH, IMT Atlantique, Université de Nantes, CNRS-IN2P3, Nantes, France
118 Suranaree University of Technology, Nakhon Ratchasima, Thailand
119 Technical University of Košice, Košice, Slovakia
120 The Henryk Niewodniczanski Institute of Nuclear Physics, Polish Academy of Sciences, Cracow, Poland
121 The University of Texas at Austin, Austin, TX, United States
122 Universidad Autónoma de Sinaloa, Culiacán, Mexico
123 Universidade de São Paulo (USP), São Paulo, Brazil
124 Universidade Estadual de Campinas (UNICAMP), Campinas, Brazil
125 Universidade Federal do ABC, Santo Andre, Brazil
126 University of Cape Town, Cape Town, South Africa
127 University of Houston, Houston, TX, United States
128 University of Jyväskylä, Jyväskylä, Finland
129 University of Liverpool, Liverpool, United Kingdom
130 University of Science and Technology of China, Hefei, China
131 University of South-Eastern Norway, Tonsberg, Norway

[132] *University of Tennessee, Knoxville, TN, United States*
[133] *University of the Witwatersrand, Johannesburg, South Africa*
[134] *University of Tokyo, Tokyo, Japan*
[135] *University of Tsukuba, Tsukuba, Japan*
[136] *Université Clermont Auvergne, CNRS/IN2P3, LPC, Clermont-Ferrand, France*
[137] *Université de Lyon, CNRS/IN2P3, Institut de Physique des 2 Infinis de Lyon , Lyon, France*
[138] *Université de Strasbourg, CNRS, IPHC UMR 7178, F-67000 Strasbourg, France*
[139] *Université Paris-Saclay Centre d'Etudes de Saclay (CEA), IRFU, Départment de Physique Nucléaire (DPhN), Saclay, France*
[140] *Università degli Studi di Foggia, Foggia, Italy*
[141] *Università di Brescia and Sezione INFN, Brescia, Italy*
[142] *Variable Energy Cyclotron Centre, Homi Bhabha National Institute, Kolkata, India*
[143] *Warsaw University of Technology, Warsaw, Poland*
[144] *Wayne State University, Detroit, MI, United States*
[145] *Westfälische Wilhelms-Universität Münster, Institut für Kernphysik, Münster, Germany*
[146] *Wigner Research Centre for Physics, Budapest, Hungary*
[147] *Yale University, New Haven, CT, United States*
[148] *Yonsei University, Seoul, Republic of Korea*

[I] Deceased.
[II] Also at: Italian National Agency for New Technologies, Energy and Sustainable Economic Development (ENEA), Bologna, Italy.
[III] Also at: Dipartimento DET del Politecnico di Torino, Turin, Italy.
[IV] Also at: M.V. Lomonosov Moscow State University, D.V. Skobeltsyn Institute of Nuclear, Physics, Moscow, Russia.
[V] Also at: Institute of Theoretical Physics, University of Wroclaw, Poland.